European Radiology (2019) 29:2107–2116
https://doi.org/10.1007/s00330-018-5750-2

COMPUTED TOMOGRAPHY

Prospective evaluation of ultra-low-dose contrast-enhanced 100-kV abdominal computed tomography with tin filter: effect on radiation dose reduction and image quality with a third-generation dual-source CT system

Pierre Leyendecker[1] · Vanina Faucher[1] · Aissam Labani[1] · Vincent Noblet[2] · François Lefebvre[3] · Paul Magotteaux[4] · Mickaël Ohana[1,2] · Catherine Roy[1,5]

Received: 6 June 2018 / Revised: 19 August 2018 / Accepted: 11 September 2018 / Published online: 15 October 2018

Abstract

Objectives To investigate the radiation dose exposure, image quality, and diagnostic performance of enhanced 100-kVp abdominopelvic single-energy CT protocol with tin filter (TF).

Methods Ninety-three consecutive patients referred for a single-phase enhanced abdominopelvic CT were prospectively included after informed consent. They underwent in addition to a standard protocol (SP) an acquisition with TF. Both examinations were performed on a third-generation dual-source CT system (DSCT), in single energy, using automatic tube current modulation, identical pitch, and identical level of iterative reconstruction. Radiation metrics were compared. Size-specific dose estimates (SSDE), contrast to noise ratio (CNR), and figure of merit (FOM) were calculated. Diagnostic confidence for the assessment of a predetermined list of abdominal lesions was rated by two independent readers.

Results The mean dose of the TF protocol was significantly lower (CDTI 1.56 ± 0.43 mGy vs. 8.13 ± 3.32, $p < 0.001$; SSDE 9.94 ± 3.08 vs. 1.93 ± 0.39, $p < 0.001$), with an effective dose close to 1 mSv (1.14 mSv ± 0.34; $p < 0.001$). TF group exhibited non-significant lower liver CNR (2.76 vs. 3.03, $p = 0.56$) and was more dose efficient (FOM 10.6 vs. 2.49/mSv, $p < 0.001$) in comparison to SP. The mean diagnostic confidence for visceral, bone, and peritoneal tumors was equivalent between both groups.

Conclusions Enhanced 100-kVp abdominopelvic CT acquired after spectral shaping with tin filtration can achieve similar diagnostic performance and CNR compared to a standard CT protocol, while reducing the radiation dose by 81%.

Key Points

- *100-kVp spectral filtration enables enhanced abdominal CT with high-dose efficiency.*
- *The radiation dose reaches the 1-mSv range.*
- *Predetermined abdominopelvic lesions can be assessed without impairing on diagnostic confidence.*

Keywords Radiation dose · Multidetector computed tomography · Abdomen

Abbreviations

ADMIRE	Advanced Modeled Iterative Reconstruction
ATVS	Automated tube voltage selection
CNR	Contrast to noise ratio
CT	Computed tomography
$CTDI_{vol}$	Volumetric CT dose index
DLP	Dose length product
DSCT	Dual-source computed tomography
ED	Effective dose
FOM	Figure of merit

✉ Pierre Leyendecker
pierre.leyendecker@chru-strasbourg.fr

[1] Service de Radiologie B, Nouvel Hôpital Civil, Hôpitaux Universitaires de Strasbourg, 1, place de l'hôpital, BP 426, 67091 Strasbourg Cedex, France

[2] iCube, Telecom Physique Strasbourg, Université de Strasbourg, CNRS UMR 7357, Illkirch, France

[3] Département de Biostatistiques, Hôpital Civil, Hôpitaux Universitaires de Strasbourg, Strasbourg, France

[4] GIE Radiologie, Institut Hospitalo-Universitaire, Institut de chirurgie guidée par l'image, Strasbourg, France

[5] Faculté de Médecine, Strasbourg, France

HU	Hounsfield unit
IR	Iterative reconstruction
ROI	Region of interest
SD	Standard deviation
SNR	Signal to noise ratio
SSDE	Size-specific dose estimates
TF	Tin filters

Introduction

Optimization of the radiation dose delivered in abdominal computed tomography (CT) imaging is of particular importance, all the more since protocols may include up to three or four acquisition phases [1, 2].

Multiple techniques for radiation dose reduction have been developed such as automatic tube current modulation, reduced tube voltage based on patient size, and iterative reconstruction algorithms [3, 4]. CT settings like tube current and tube voltage can be tailored to the patients' morphotype and to the clinical indication to better manage the radiation dose; routine abdominopelvic CT scans are usually performed at 100–140 kVp based on automatic tube voltage selection techniques [5].

On a third-generation dual-source CT system (DSCT), an additional way of reducing the radiation dose delivered is represented by tin filters (TF). Placed in front of both X-ray tubes, applying TF will absorb the low-energy photons that contribute little to image quality but do increase the dose of radiation that a patient receives, due mainly to photoelectric effect. Therefore, an additional built-in 0.6-mm thick TF will, at a fixed tube voltage of 100 kVp, remove the bulk of lower energy photons, resulting in a mean photon energy of 78.7 keV [6]. This is significantly higher than the mean energy of a standard 100-kVp examination at 66.4 keV [6], suggesting a substantially reduced radiation dose. The approach of using TF, called "spectral filtration" or "spectral shaping," was initially assessed in non-contrast chest DSCT studies [6, 7] taking advantage of the natural high contrast of these anatomical structures [8], but have never been studied in contrast-enhanced abdominal CT imaging.

The question of how much dose reduction is reasonable to achieve is highly task and patient dependent. This is particularly relevant in oncologic abdominopelvic follow-up examinations, which require a high accuracy for the assessment of target lesions; an underestimation of these lesions could have a significant clinical impact in this context.

The objectives of this study were therefore to investigate the radiation dose exposure and quantitative image quality of enhanced abdominopelvic CT examinations acquired at 100 kVp with spectral shaping in comparison to a standard acquisition in the same patient and to estimate the diagnostic performance of this technique for the assessment of a predetermined list of abdominopelvic lesions.

Material and methods

Patients

This prospective single-center study was approved by our institutional review board and complies with the Declaration of Helsinki. Informed consent was obtained from all participating patients.

From January to September 2017, all consecutive patients referred to our department for a clinically indicated enhanced abdominopelvic CT examination, in the context of an oncological follow-up, were prospectively included. There was no other inclusion criterion. Exclusion criteria were the usual contraindications to iodine contrast media injection (MDRD eGFR lower than 30 mL/min, proven allergy to iodine contrast media), pregnancy, and the inability to give informed consent.

Examination technique

All examinations were acquired on a third-generation DSCT (Siemens SOMATOM Force, Siemens Healthineers). Included patients underwent two successive helical scans within the same examination, always in the same order: one ultra-low-dose TF acquisition using TF placed in front of both tubes, followed by one standard-dose acquisition. The time interval between the two scans was 5 s maximum due to the table repositioning and rebreathing.

The CT acquisition scanning parameters for both spectral filtration and control group are summarized in Table 1. The only difference was the use of TF with 100 kVp compared to an automatic tube voltage selection with a range of 90 to 150 kVp. All patients were examined using automatic tube current modulation (ATCM) for effective mAs (CareDose 4D, Siemens Healthineers).

Contrast enhancement was achieved by injecting 1.0 mL/kg of non-ionic low-osmolar iodinated contrast material (300 mgI/mL) via an intercubital vein at a flow rate of a 2.5 mL/s using a dual-syringe power injector without saline flush.

In all patients, the scan range was kept identical for both acquisitions and covered the entire abdominopelvic cavity, extending from the upper level of the liver to the level of ischion. All patients were asked to stand a deep-inspiration breath hold for each acquisition. The complete scan duration for each protocol is shown in Table 1.

Image reconstruction

All images were reconstructed with a slice thickness of 2.0 mm in the axial plane using a soft tissue kernel with the same iterative reconstruction techniques (Adaptative Model-based Iterative Reconstruction, ADMIRE, Siemens Healthineers) set at a level of 4.

Table 1 CT acquisition scanning parameters for both spectral filtration and control group

	Standard protocol (SP)	Tin filter (TF)
Scanner	SOMATOM Force*	SOMATOM Force*
kV	Automatic tube voltage selection (CareDose 4D®). 90, 100, 110, 120, 150 kVp	Sn100 kVp (dedicated tin filter 0.6 mm thickness)
mAs	Automatic tube current modulation (CareDose 4D®) Ref. mAs 233 ± 68† Eff. mAs 195.6 ± 55.5†	Automatic tube current modulation (CareDose 4D®) Ref. mAs 396 ± 17.8† Eff. mAs 450.2 ± 123.4†
Iterative Reconstruction	Iterative reconstruction ADMIRE® strength 4	Iterative reconstruction ADMIRE® strength 4
Rotation time (s)	0.5	0.5
Collimation width (mm)	1.2	1.2
Detector rows	48	48
Pitch	0.8	0.8
Complete scan duration (s)	5	5

ADMIRE Advanced Modeled Iterative Reconstruction

*SIEMENS Healthineers

† Data are mean ± standard deviation calculated over all patients

The images were anonymized and randomized, with TF and control examinations merged and randomized together, before being exported to an offline workstation for all data analysis.

Objective image quality assessment

A quantitative analysis was performed in different anatomical regions. CT values (HU) and image noise (SD of measured HU values) were determined on the reconstructed 2-mm axial CT images using equal ROIs (1.1 cm^2), placed within the liver, the abdominal aorta, the spinal erector muscles, and the subcutaneous fat. Each ROI was placed in an identical or nearly identical segment by the same operator (P.L., radiologist with 5 years of experience in CT imaging). Image noise was considered the standard deviation of CT attenuation measured within the air space outside of the anterior pelvic wall. For each ROI, the mean and standard deviation of the HU values were determined. Finally, signal to noise ratio (SNR) and contrast to noise ratio (CNR) were calculated for each image dataset using the following equations: SNR = (mean_interested area/SD_air); CNR = (mean_interested area-mean_muscle)/(SD_interested area) [9].

A figure of merit (FOM) was calculated as CNR^2/effective dose [10] to compare the dose efficiency between the two acquisition protocols.

Subjective image quality assessment

Two independent readers (A.L., radiologist with 10 years of experience in CT, reader 1, and V.F., radiologist with 18 years of experience in CT, reader 2), who were blinded to the acquisition protocol, independently rated the overall image quality on a 5-point Likert scale (1, unacceptable; 2, fair; 3, moderate; 4, good; 5 excellent) as described for whole-body staging CT examinations in the European Guidelines on Quality Criteria for CT [11]. Additionally, image noise was subjectively assessed using another 5-level Likert scale (1, unacceptable image noise; 2, above average noise; 3, average image noise; 4, less than average image noise; 5, minimal image noise).

Diagnostic performances

For each presented acquisition, both readers had to independently assess the presence of five predetermined abdominopelvic lesions: visceral tumor (whatever the localization), peritoneal tumor, bone tumor, significant post-surgical complication, and infectious abnormalities.

Each item was graded using a confidence index (0, not confident; 1, moderately confident; 2, quite confident, 3, highly confident) in confirming or excluding the lesion with the given image quality, regardless of whether the patient had this specific lesion.

Radiation dose assessment

Recorded dose parameters for each patient and for each acquisition were the volume CT dose index ($CTDI_{vol}$), the dose-length product (DLP), the effective tube current (mAs), and the tube voltage (kVp), as obtained from the CT dose report and DICOM data.

Effective dose was estimated by multiplying the DLP by a standard conversion factor for adult abdominopelvic CT of 0.017 mSv/mGy.cm [12]. Anthropometric data (transversal and anteroposterior diameters) were collected, and the effective diameter (EDiam) was calculated based on the

anteroposterior (AP) and transverse (T) diameter measured at the celiac trunk as follows: EDiam = √(APxT) [13]. Based on the EDiam, size-specific dose estimates (SSDEs) were calculated using the adult size-specific conversion factor f_{size} (SSDE = f_{size}.CTDI$_{vol}$) [14].

Statistical analysis

Statistical analyses were performed using R 3.4.3 Software (R Foundation for Statistical Computing) at a significance level of 0.05.

Data are displayed as mean ± SD and were tested for Gaussian distribution using the Shapiro-Wilk test and quantile-quantile plot.

Student's *t* test or Mann-Whitney-Wilcoxon tests were used to compare quantitative parameters, especially radiation metrics between the two acquisition protocols.

Statistical correlation tests used Pearson and Spearman coefficient.

Kappa statistics were used for overall inter-rater agreement in both groups.

Results

Demographics

Ninety-three consecutive patients (31 females, 62 males; mean age 66.1 ± 10.7 years old) were ultimately included. They had a mean abdominal effective diameter of 29.4 ± 3.6 cm.

Radiation dose

The mean DLP was 399.5 ± 177.7 mGy.cm in the control group (SP) and 75.9 ± 22.9 mGy.cm in the TF group ($p < 0.001$, Table 2). The mean values for CTDI$_{vol}$ and SSDE were 8.13 ± 3.32 and 9.94 ± 3.08 and 1.56 ± 0.43 and 1.93 ± 0.39 mGy, respectively, $p < 0.001$ for both), corresponding to an 81% decrease in dose using TF (Fig. 1). The effective dose calculated for TF was close to 1 mSv. Regardless of patients' morphotype, the TF radiation dose is mainly maintained between 1 and 2 mSv while it increases exponentially with the effective diameter for SP (Fig. 2). For both TF and SP, the coefficient of determination R^2 is higher with exponential than linear models, meaning that the dose increases with the effective diameter exponentially. For the SP protocol, the equation of the curve estimated is $y = 0.4561.e^{0.0849x}$ with a coefficient of determination $R^2 = 0.624$, and for the TF protocol, the equation of the curve estimated is $y = 0.1537.e^{0.0666x}$ with a coefficient of determination $R^2 = 0.665$. It is interesting to note the higher exponential coefficient for SP than TF reflecting the higher increase of the dose according to the effective diameter.

Objective image quality and dose efficiency

The background noise measured was comparable (19.8 ± 17.9 and 19.0 ± 16.4 for SP and TF, respectively, $p = 0.63$, Table 3).

There was no statistically significant difference for the mean CNR within the abdominal aorta and the liver between both groups (6.09 ± 1.92 and 3.03 ± 1.49 vs. 5.92 ± 2.41 and 2.76 ± 1.65, $p = 0.38$ and 0.56, respectively). The mean FOM was 8.69 ± 7.09 mSv^{-1} for the aorta and 2.49 ± 2.44 mSv^{-1} for the liver in the control group and 39.5 ± 42.2 mSv^{-1} and 10.6 ± 11.6 mSv^{-1} for the TF group, respectively ($p < 0.001$), corresponding to a mean increase of a factor of 4.5 for the TF.

Subjective image quality assessment

The mean overall image quality rating was higher in the control group (4.29 ± 0.32 vs. 3.54 ± 0.47, $p < 0.01$).

Similarly, the mean score for image noise was better in the SP group in comparison to that in the TF group (4.10 ± 0.39 vs. 3.27 ± 0.40, $p = 0.01$).

Diagnostic confidence

The distribution of diagnostic confidence ratings for the two readers is shown in Table 4. No statistically significant

Table 2 Radiation metrics of both groups

	Standard protocol ($n = 93$)	Tin filter ($n = 93$)	*p* value*
CTDI$_{vol}$ (mGy)	8.13 ± 3.32 (6.08–9.37)	1.56 ± 0.43 (1.23–1.78)	< 0.001
DLP (mGy.cm)	399.5 ± 177.7 (276–432)	75.9 ± 22.9 (58.2–86.8)	< 0.001
Effective dose (mSv)	5.99 ± 2.66 (4.14–6.48)	1.14 ± 0.34 (0.87–1.30)	< 0.001
Effective mAs	195.6 ± 55.5 (151–233)	450.2 ± 123.4 (355–513)	< 0.001
SSDE (mGy)	9.94 ± 3.08 (7.94–11.2)	1.93 ± 0.39 (1.70–2.13)	< 0.001

Data are mean ± standard deviation with the interquartile range in parenthesis

CTDI$_{vol}$ computed tomography dose index, *DLP* dose length product, *SSDE* size-specific dose estimates

**p* values are a comparison between both protocols with and without spectral filtration. They were calculated by using Student's *t* test

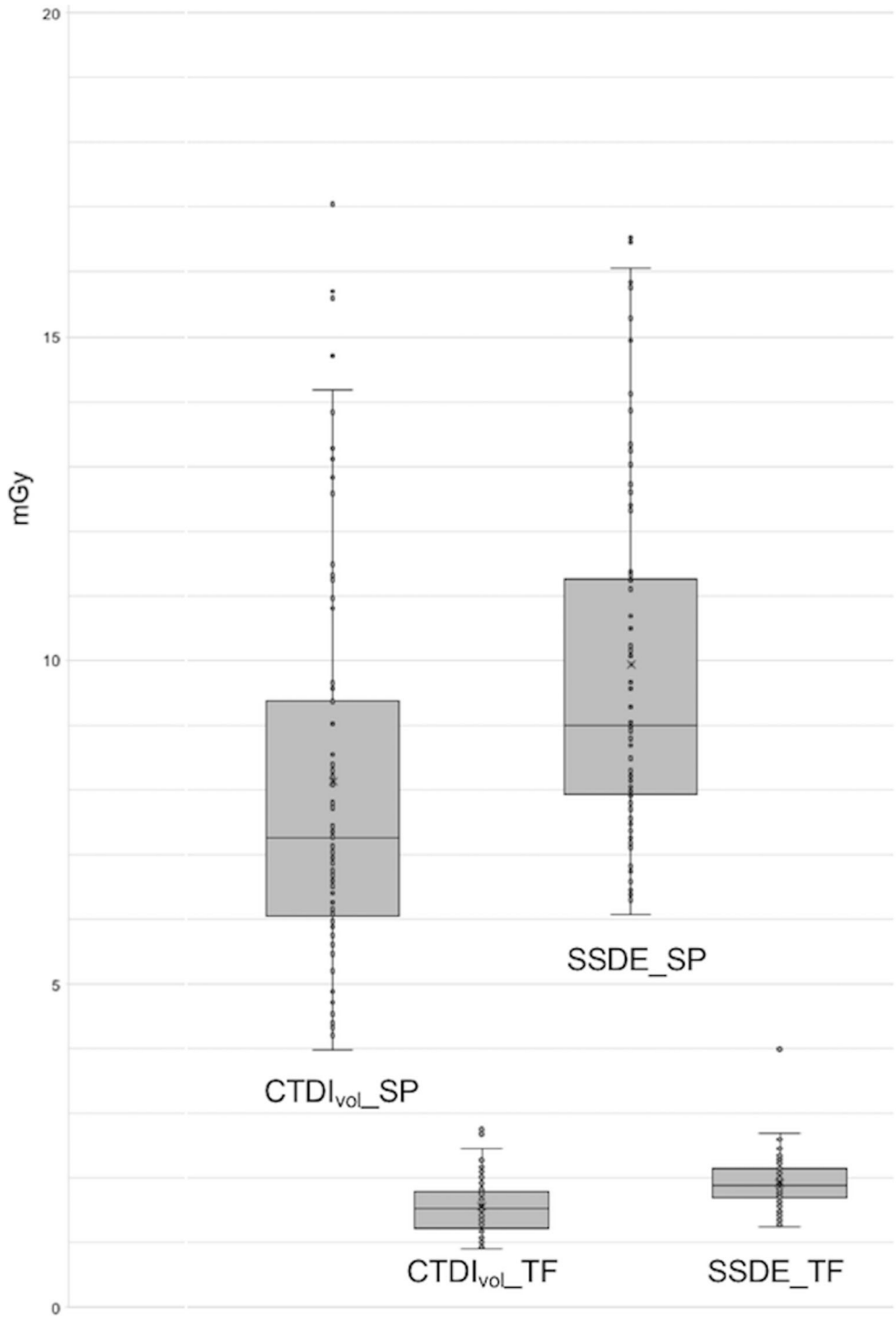

Fig. 1 $CDTI_{vol}$ and SSDE for CT without (SP) and with spectral filtration (TF). Box-and-whisker diagrams show mean values ± standard deviation and minimum and maximum values.

differences were found between the control group and spectral filtration group for the assessment of evaluated abdominal abnormalities (average reader 1, 2.82 ± 0.26 vs. 2.77 ± 0.22, $p = 0.21$; average reader 2, 2.85 ± 0.22 vs. 2.78 ± 0.26, $p = 0.053$), with an overall confidence that was constantly over 2.5 out of 3 (i.e., quite to highly confident). In both groups, the lowest confidence was attributed to the assessment of visceral tumor and the highest confidence to the assessment of bone metastases.

Reader and method agreements

The intra-reader agreement was good to high for reader 2 and moderate to good for reader 1 (Table 5).

The inter-reader agreement for the assessment of tumoral lesions (visceral, peritoneal, and bone) was 63% for SP and even higher at 65% for TF ($p < 0.01$). For surgical complication, the inter-reader agreement was higher for the TF protocol in

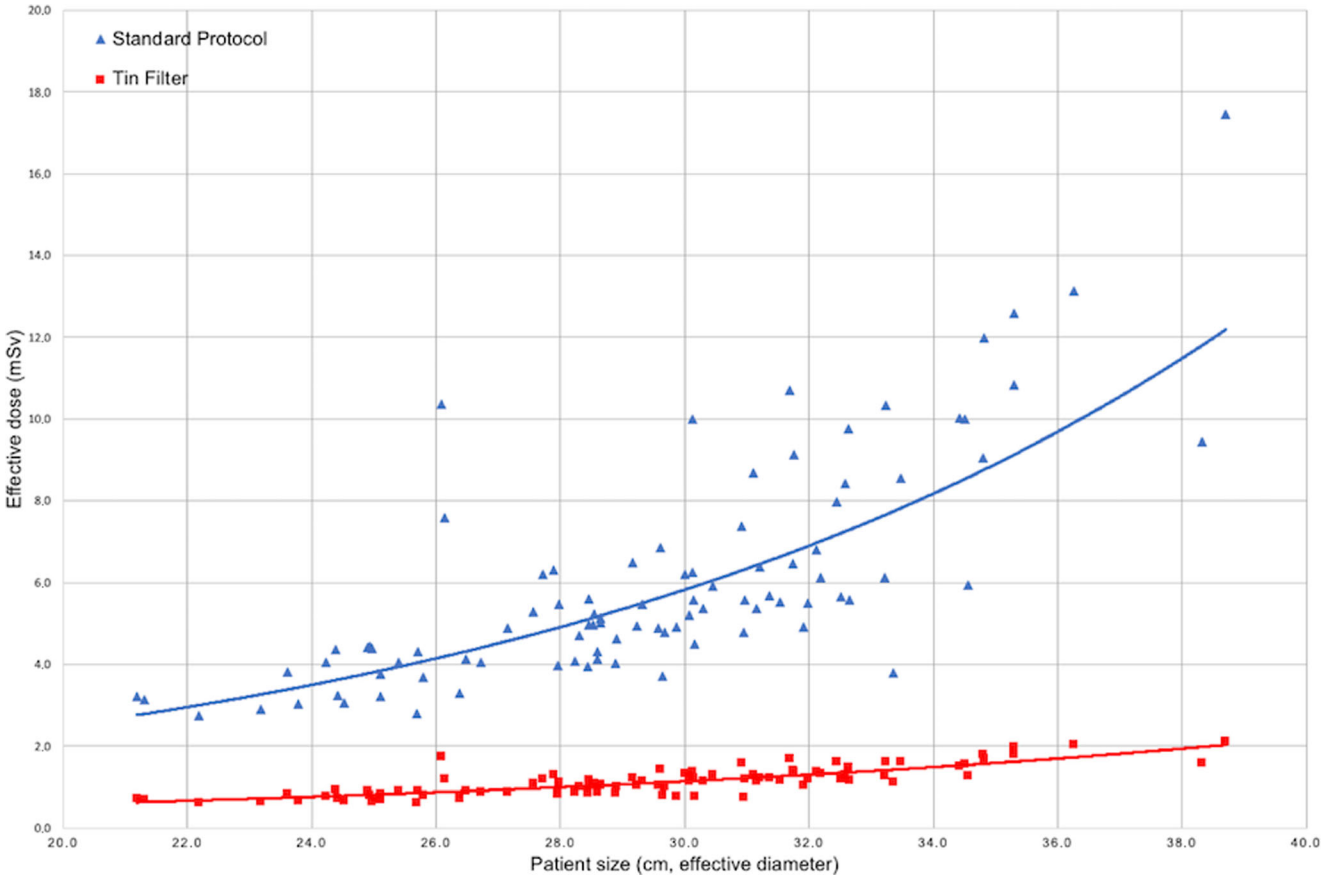

Fig. 2 Distribution of effective dose plotted against the patient size (effective diameter). Note the higher increase of the dose for SP than TF according to the effective diameter. Exponential growth curves estimated are shown for both protocols

comparison to that for the SP protocol ($\kappa = 0.53$ and 0.47 respectively, $p < 0.01$).

Kappa of inter-method agreement ranged from 0.78 (tumor lesions) to 0.48 (infectious pathology). The risk to misestimate the presence or absence of abdominal pathologies evaluated was close to 0, with a peak for infectious pathology (0.06, $p = 0.13$), suggesting that the difference observed in the inter-reader agreement is probably not related to the different acquisition protocols.

Discussion

Our study demonstrates that low-dose enhanced abdominal computed tomography using 100 kV with TF as spectral shaping allows a significant reduction of radiation exposure by 81% compared to a standard CT acquisition. The mean effective dose was close to 1 mSv and comparable to the radiation exposure of an abdominal standard radiography [15].

Table 3 Assessment of objective image quality

	Standard protocol ($n = 93$)	Tin filter ($n = 93$)	$p^{\dagger}$
CNR abdominal aorta	6.09 ± 1.92	5.92 ± 2.41	0.38
SNR abdominal aorta	13.6 ± 7.53	10.8 ± 5.51	0.13
FOM abdominal aorta (mSv^{-1})	8.69 ± 7.09	39.5 ± 42.2	< 0.001
CNR liver	3.03 ± 1.49	2.76 ± 1.65	0.56
SNR liver	8.82 ± 4.72	7.30 ± 3.69	0.28
FOM liver (mSv^{-1})	2.49 ± 2.44	10.6 ± 11.6	< 0.001
Background noise[‡]	19.8 ± 17.9	19.0 ± 16.4	0.63

Data are mean ± standard deviation

CNR contrast to noise ratio, *SNR* signal to noise ratio, *FOM* figure of merit

[†] p values are a comparison between both protocols with and without spectral filtration. They were calculated by using Student's t test

[‡] Background noise is calculated as the mean of standard deviation of CT attenuation in ROIs placed within the air space outside of the anterior pelvic wall

Table 4 Subjective assessment of diagnostic confidence

Diagnostic confidence		Reader 1			Reader 2		
		SP‡	TF†	*p**	SP‡	TF†	*p**
Visceral tumor	Confidence	2.67 ± 0.55	2.60 ± 0.51	0.41	2.70 ± 0.48	2.50 ± 0.58	0.01
Peritoneal tumor	Confidence	2.88 ± 0.32	2.78 ± 0.41	0.07	2.83 ± 0.48	2.77 ± 0.49	0.45
Bone tumor	Confidence	2.93 ± 0.29	2.91 ± 0.28	0.61	3 ± 0	2.99 ± 0.10	0.32
Infectious abnormalities	Confidence	2.77 ± 0.49	2.76 ± 0.47	0.88	2.86 ± 0.38	2.81 ± 0.45	0.38
Post-surgical complication	Confidence	2.81 ± 0.41	2.78 ± 0.44	0.61	2.88 ± 0.36	2.85 ± 0.36	0.54
	Average	2.02 ± 0.26	2.77 ± 0.22	0.21	2.85 ± 0.22	2.78 ± 0.26	0.053

Data are mean ± standard deviation

‡ *SP* standard protocol

† *TF* tin filter protocol

**p* values were calculated by using Student's *t* test

Despite a non-significant lower subjective overall image quality, the observed differences between both readers for confirming or excluding spectrum of abdominal pathologies were not attributable to the protocol used. This is also supported by the fact that objective metrics like background noise, CNR, and SNR within anatomical structures were similar between both groups.

Various techniques for radiation dose reduction have been developed to minimize abdominopelvic dose exposure. Since the introduction of MDCT, the total number and clinical indications for CT examinations have grown steadily. CT is by far the largest contributor to medical radiation exposure among the US and European population [16]. This explains the emergence of low-dose CT protocols. Traditionally, the highest dose savings was achieved by lowering the tube voltage [17, 18]. The expected dose radiation reduction with a technique of automatic tube current modulation in combination with a technique of automatic tube voltage selection (ATVS) is about 42% [19]. Lowering the tube voltage leads to a compensatory increase in tube current because both parameters depend on each other [10, 18, 19].

Iterative reconstruction algorithms allow a further radiation dose reduction while maintaining a low level of noise [20–23]. Park et al investigated in a simulation study an abdominopelvic exploration CT with less than 1 mSv for suspected appendicitis in young adults using an iterative reconstruction [24]. The 1.0-mSv appendical CT was non-inferior to the 2.0-mSv CT in terms of diagnostic performance for both abdominal and non-abdominal radiologists. However, previous iterative algorithms were prone to reduce subjective image quality due to an artificial "plastic" appearance that has been described by various authors [25, 26].

Another way to reduce the dose appears in the third-generation DSCT with the TF. Initially, the tin filter was used to allow a better spectral separation when performing dual-energy CT examination [27]. These techniques can also be utilized in single energy mode to optimize the X-ray spectrum in a process known as "spectral shaping" [26–32]. The additional prefiltration with a tin filter hardens the energy spectrum of the X-ray beam, and less low-energy radiation is delivered to the patient.

Suntharalingam et al demonstrated recently that whole-body low-dose CT using spectral shaping with Sn100 for the

Table 5 Kappa agreements for both readers and methods

	Intra-reader agreement				Inter-reader agreement			Inter-method agreement	
	Kappa	*p* value*	Kappa	*p* value*	Kappa	Kappa	*p* value*	Kappa	*p* value*
	Reader 1		Reader 2		SP‡	TF†			
Visceral tumor	0.69	< 0.01	0.89	< 0.01	0.63	0.65	< 0.01	0.78	< 0.01
Peritoneal tumor	0.58	< 0.01	0.66	< 0.01	0.24	0.38	< 0.01	0.60	< 0.01
Bone Tumor	0.26	< 0.01	1	< 0.01	0	0	–	0.43	< 0.01
Infectious abnormalities	0.47	< 0.01	0.49	< 0.01	0	0	–	0.48	< 0.01
Post-surgical complication	0.57	< 0.01	0.94	< 0.01	0.47	0.53	< 0.01	0.71	< 0.01

Data shown are Cohen weighted kappa

‡ *SP* standard protocol

† *TF* tin filter protocol

*The chi-square test was used to test for statistical significance obtained from Pearson coefficients

assessment of osteolytic lesions in patients with multiple myeloma can obtain sufficient image quality while reducing the radiation dose by approximately 74% [33]. In thorax imaging, 100-kVp spectral shaping on a third-generation DSCT allows 90% dose reduction when compared to a standard low kV protocol without spectral shaping [6].

In the field of abdominal imaging, only a few studies have evaluated the benefit of the TF and only for low-dose non-contrast-enhanced abdominal CT [34, 35]. Dewes et al compared three different protocols for urolithiasis, one using tin filter at 150 kVp (Sn150) on a third-generation DSCT, one without filtering using ATVS on the same device, and one on a second-generation DSCT without filtering [35]. The maximal dose reduction obtained is 36% when using an additional shaping of a 150-kVp source spectrum in comparison to the standard protocol without filtering on the same device. An identical protocol was used for virtual computed tomography colonography with a total amount of effective dose of below 1 mSv without impairing on 2D or 3D image quality [36]. It should be emphasized that most of these prior studies have compared protocols based on second and third DSCT with different iterative reconstruction techniques.

To the best of our knowledge, this is the first study to assess an ultra-low-dose protocol using Sn100 kVp for contrast-enhanced abdominopelvic CT imaging.

In comparison to a standard protocol without TF, the exploration with TF shifts the mean energy of the spectrum from 66.4 to 78.4 keV [27]. The use of a Sn150-kVp tube voltage does not appear suitable when dealing with enhanced abdominopelvic examinations, due to an increase of the Compton effect resulting in a decrease of contrast resolution. It could be promising to reduce the tube voltage, for example, down to Sn90kVp or Sn70kVp, using spectral shaping for contrast-enhanced abdominopelvic CT for small or pediatric patients. However, lower levels of tube voltage likely these are not yet calibrated for this third-generation DSCT.

We demonstrate that the inter-method agreement is good for confirming or excluding a wide spectrum of abdominal lesions, despite a slight and clinically acceptable degradation of objective and subjective image quality in the TF group. The diagnostic confidence and the overall image quality remain good or very good, which advocates of the use of this low-dose protocol in clinical routine. Moreover, there was no difference in background noise between the two protocols which is due to a

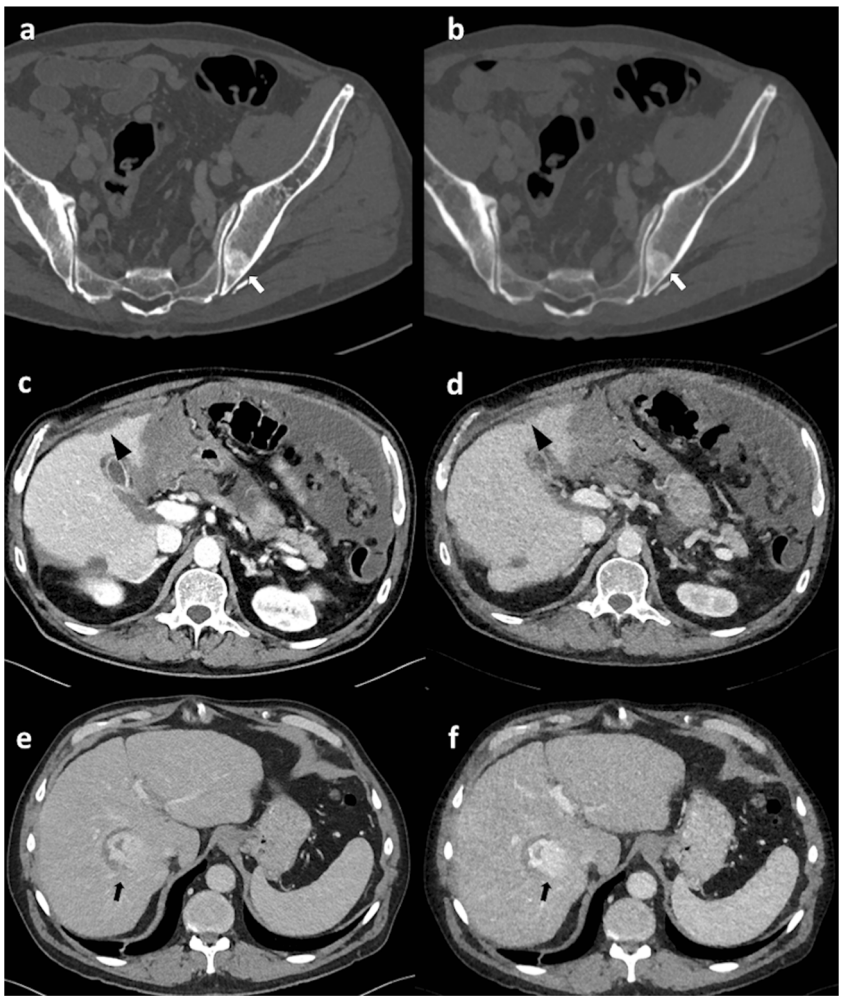

Fig. 3 Examples of third-generation dual-source computed tomography clinical applications without (**a**, **c**, **e**) or with (**b**, **d**, **f**) Sn100 spectral shaping in three different patients. Left iliac metastasis is shown (**a**, **b**) with respectively $CTDI_{vol}$ of 5.50 and 1.19 mGy. Peritoneal metastasis (**c**, **d**) with respectively $CTDI_{vol}$ of 7.42 versus 1.59 mGy. Note that the image contrast without filtration is higher (helical scan at 90 kVp instead of Sn100 kVp). Liver hypervascular lesion (**e**, **f**) with respectively $CTDI_{vol}$ of 12.6 and 1.93 mGy. Note that the lesion is seen with a higher contrast with the tin filter exploration due to the lower tube voltage in this case in comparison to the control group (100 vs. 150 kVp)

higher reference tube current with spectral shaping [37] and the use of ATCM that adjust the tube current such that the image noise remains relatively constant over the complete scan range.

Our study has some potential limitations which have to be considered.

First, the assessment of objective image quality, i.e., the CNR ratio, is a variable of the tube voltage, and this parameter was not kept constant between both groups. Indeed, while the tube voltage is fixed at 100 kVp in the TF group, we chose to use automatic tube voltage selection depending on patient's morphotype in the SP group. Thus, a higher contrast might be obtained when a tube voltage lower than 100 kV is selected by ATVS. This represents over half of the patients included (52 of 93 patients). That would favor the SP group and could partially explain the higher objective quality of some explorations in this group. Some clinical examples reflecting the contrast changes are shown in Fig. 3.

Second, we assessed only the diagnostic confidence and not the diagnostic accuracy of spectral filtration in some abdominal findings. Further studies with a larger patient population should be performed to evaluate this protocol in abdominal pathology, especially in the emergency setting, and not only in oncology.

Third, slight differences in image quality between the two protocols, like a blurring appearance for TF images, may lead to imperfect blinding of the readers. Thus, the choice of a smoother reconstruction kernel for TF exploration (Bf32 instead of Br40 for SP) may have compromised the analyses of bone structures. A complementary study should evaluate the subjective image quality by using different reconstruction kernels depending on organs studied.

Lastly, the minimum time period of 5 s between the end of the first acquisition (TF) and the second one (SP) that starts sequentially might slightly overestimate CNR particularly within vascular structures in favor of TF. We do think that this time period could not significantly affect the objective or subjective image quality evaluation of these portal phase examinations.

In conclusion, we found that enhanced contrast abdominopelvic CT using spectral filtration was significantly more dose efficient than CT without spectral filtration. Achieving similar background noise and objective image quality, spectral filtration provided sufficient diagnostic confidence for the assessment of a spectrum of abdominal abnormalities, while substantially reducing the radiation dose by 81%.

Compliance with ethical standards

Guarantor The scientific guarantor of this publication is Catherine Roy, MD, PhD.

Conflict of interest The authors declare that they have no conflict of interest.

Statistics and biometry François Lefebvre, MD, kindly provided statistical advice for this manuscript.

No complex statistical methods were necessary for this paper.

Informed consent Written informed consent was obtained from all patients in this study.

Ethical approval Institutional Review Board approval was obtained.

Methodology
- Prospective
- Case-control study
- Performed at one institution

References

1. Goshima S, Kanematsu M, Kondo H et al (2006) Pancreas: optimal scan delay for contrast-enhanced multi-detector row CT. Radiology 241:167–174. https://doi.org/10.1148/radiol.2411051338
2. McTavish JD, Jinzaki M, Zou KH, Nawfel RD, Silverman SG (2002) Multi-detector row CT urography: comparison of strategies for depicting the normal urinary collecting system. Radiology 225: 783–790. https://doi.org/10.1148/radiol.2253011515
3. McNitt-Gray MF (2002) AAPM/RSNA Physics Tutorial for Residents: Topics in CT. Radiation dose in CT. Radiographics 22: 1541–1553.
4. Tamm EP, Rong XJ, Cody DD, Ernst RD, Fitzgerald NE, Kundra V (2011) Quality initiatives: CT radiation dose reduction: how to implement change without sacrificing diagnostic quality. Radiographics 31:1823–1832. https://doi.org/10.1148/rg.317115027
5. Hough DM, Fletcher JG, Grant KL et al (2012) Lowering kilovoltage to reduce radiation dose in contrast-enhanced abdominal CT: initial assessment of a prototype automated kilovoltage selection tool. AJR Am J Roentgenol 199:1070–1077. https://doi.org/10.2214/AJR.12.8637
6. Haubenreisser H, Meyer M, Sudarski S, Allmendinger T, Schoenberg SO, Henzler T (2015) Unenhanced third-generation dual-source chest CT using a tin filter for spectral shaping at 100kVp. Eur J Radiol 84:1608–1613. https://doi.org/10.1016/j.ejrad.2015.04.018
7. Braun FM, Johnson TR, Sommer WH, Thierfelder KM, Meinel FG (2015) Chest CT using spectral filtration: radiation dose, image quality, and spectrum of clinical utility. Eur Radiol 25:1598–1606. https://doi.org/10.1007/s00330-014-3559-1
8. Ludes C, Schaal M, Labani A, Jeung MY, Roy C, Ohana M (2016) Ultra-low dose chest CT: the end of chest radiograph? Presse Med 1983 45:291–301. https://doi.org/10.1016/j.lpm.2015.12.003
9. Szucs-Farkas Z, Strautz T, Patak MA, Kurmann L, Vock P, Schindera ST (2009) Is body weight the most appropriate criterion to select patients eligible for low-dose pulmonary CT angiography? Analysis of objective and subjective image quality at 80 kVp in 100 patients. Eur Radiol 19:1914–1922. https://doi.org/10.1007/s00330-009-1385-7
10. Marin D, Nelson RC, Schindera ST et al (2010) Low-tube-voltage, high-tube-current multidetector abdominal CT: improved image quality and decreased radiation dose with adaptive statistical iterative reconstruction algorithm–initial clinical experience. Radiology 254:145–153. https://doi.org/10.1148/radiol.09090094
11. (1998) Danish Society of Radiology website. European guidelines on quality criteria for computed tomography. http://www.drs.dk/guidelines/ct/quality/htmlindex.htm
12. Deak PD, Smal Y, Kalender WA (2010) Multisection CT protocols: sex- and age-specific conversion factors used to determine effective dose from dose-length product. Radiology 257:158–166. https://doi.org/10.1148/radiol.10100047

13. Christner JA, Braun NN, Jacobsen MC, Carter RE, Kofler JM, McCollough CH (2012) Size-specific dose estimates for adult patients at CT of the torso. Radiology 265:841–847. https://doi.org/10.1148/radiol.12112365
14. McCollough C, Bakalyar DM, Bostani M et al (2014) Use of water equivalent diameter for calculating patient size and size-specific dose estimates (SSDE) in CT: the report of AAPM task group 220. AAPM Rep 2014:6–23
15. Mettler FA Jr, Huda W, Yoshizumi TT, Mahesh M (2008) Effective doses in radiology and diagnostic nuclear medicine: a catalog. Radiology 248:254–263. https://doi.org/10.1148/radiol.2481071451
16. Mettler FA Jr, Bhargavan M, Faulkner K et al (2009) Radiologic and nuclear medicine studies in the United States and worldwide: frequency, radiation dose, and comparison with other radiation sources–1950–2007. Radiology 253:520–531. https://doi.org/10.1148/radiol.2532082010
17. Nyman U, Björkdahl P, Olsson ML, Gunnarsson M, Goldman B (2012) Low-dose radiation with 80-kVp computed tomography to diagnose pulmonary embolism: a feasibility study. Acta Radiol 1987 53:1004–1013. https://doi.org/10.1258/ar.2012.120327
18. Knipp D, Lane BF, Mitchell JW, Daly BD (2017) Computed tomographic angiography of the abdomen and pelvis in azotemic patients utilizing 80-kV(p) technique and reduced dose iodinated contrast: comparison with routine 120-kV(p) technique. J Comput Assist Tomogr 41:141–147. https://doi.org/10.1097/RCT.0000000000000478
19. Mayer C, Meyer M, Fink C et al (2014) Potential for radiation dose savings in abdominal and chest CT using automatic tube voltage selection in combination with automatic tube current modulation. AJR Am J Roentgenol 203:292–299. https://doi.org/10.2214/AJR.13.11628
20. Euler A, Stieltjes B, Szucs-Farkas Z et al (2017) Impact of model-based iterative reconstruction on low-contrast lesion detection and image quality in abdominal CT: a 12-reader-based comparative phantom study with filtered back projection at different tube voltages. Eur Radiol 27:5252–5259. https://doi.org/10.1007/s00330-017-4825-9
21. Holmquist F, Nyman U, Siemund R3, Geijer M, Söderberg M (2015) Impact of iterative reconstructions on image noise and low-contrast object detection in low kVp simulated abdominal CT: a phantom study. Acta Radiol 1987. https://doi.org/10.1177/0284185115617347
22. McCollough CH, Bartley AC, Carter RE et al (2017) Low-dose CT for the detection and classification of metastatic liver lesions: results of the 2016 Low Dose CT Grand Challenge. Med Phys 44:e339–e352. https://doi.org/10.1002/mp.12345
23. Kataria B, Althén JN, Smedby Ö, Persson A, Sökjer H, Sandborg M (2018) Assessment of image quality in abdominal CT: potential dose reduction with model-based iterative reconstruction. Eur Radiol. https://doi.org/10.1007/s00330-017-5113-4
24. Park JH, Jeon JJ, Lee SS et al (2017) Can we perform CT of the appendix with less than 1 mSv? A de-escalating dose-simulation study. Eur Radiol. https://doi.org/10.1007/s00330-017-5159-3
25. Vonder M, Pelgrim GJ, Huijsse SE et al (2017) Feasibility of spectral shaping for detection and quantification of coronary calcifications in ultra-low dose CT. Eur Radiol 27:2047–2054. https://doi.org/10.1007/s00330-016-4507-z
26. Leipsic J, Labounty TM, Heilbron B et al (2010) Estimated radiation dose reduction using adaptive statistical iterative reconstruction in coronary CT angiography: the ERASIR study. AJR Am J Roentgenol 195:655–660. https://doi.org/10.2214/AJR.10.4288
27. Primak AN, Ramirez Giraldo JC, Liu X, Yu L, McCollough CH (2009) Improved dual-energy material discrimination for dual-source CT by means of additional spectral filtration. Med Phys 36:1359–1369. https://doi.org/10.1118/1.3083567
28. Weis M, Henzler T, Nance JW Jr et al (2017) Radiation dose comparison between 70 kVp and 100 kVp with spectral beam shaping for non-contrast-enhanced pediatric chest computed tomography: a prospective randomized controlled study. Invest Radiol 52:155–162. https://doi.org/10.1097/RLI.0000000000000325
29. May MS, Brand M, Lell MM, et al (2017) Radiation dose reduction in parasinus CT by spectral shaping. Neuroradiology https://doi.org/10.1007/s00234-016-1780-0
30. Lell MM, May MS, Brand M et al (2015) Imaging the parasinus region with a third-generation dual-source CT and the effect of tin filtration on image quality and radiation dose. AJNR Am J Neuroradiol 36:1225–1230. https://doi.org/10.3174/ajnr.A4270
31. Martini K, Barth BK, Nguyen-Kim TD, Baumueller S, Alkadhi H, Frauenfelder T (2016) Evaluation of pulmonary nodules and infection on chest CT with radiation dose equivalent to chest radiography: prospective intra-individual comparison study to standard dose CT. Eur J Radiol 85:360–365. https://doi.org/10.1016/j.ejrad.2015.11.036
32. Gordic S, Morsbach F, Schmidt B et al (2014) Ultralow-dose chest computed tomography for pulmonary nodule detection: first performance evaluation of single energy scanning with spectral shaping. Invest Radiol 49:465–473. https://doi.org/10.1097/RLI.0000000000000037
33. Suntharalingam S, Mikat C, Wetter A, et al (2018) Whole-body ultra-low dose CT using spectral shaping for detection of osteolytic lesion in multiple myeloma. Eur Radiol https://doi.org/10.1007/s00330-017-5243-8
34. Zhang GM, Shi B, Sun H et al (2017) High-pitch low-dose abdominopelvic CT with tin-filtration technique for detecting urinary stones. Abdom Radiol (NY) 42:2127–2134. https://doi.org/10.1007/s00261-017-1103-x
35. Dewes P, Frellesen C, Scholtz JE et al (2016) Low-dose abdominal computed tomography for detection of urinary stone disease - impact of additional spectral shaping of the X-ray beam on image quality and dose parameters. Eur J Radiol 85:1058–1062. https://doi.org/10.1016/j.ejrad.2016.03.016
36. Seuss H, Janka R, Hammon M, Cavallaro A, Uder M, Dankerl P (2018) Virtual computed tomography colonography: evaluation of 2D and virtual 3D image quality of sub-mSv examinations enabled by third-generation dual source scanner featuring tin filtering. Acad Radiol https://doi.org/10.1016/j.acra.2017.12.014
37. Bodelle B, Fischbach C, Booz C et al (2017) Single-energy pediatric chest computed tomography with spectral filtration at 100 kVp: effects on radiation parameters and image quality. Pediatr Radiol 47:831–837. https://doi.org/10.1007/s00247-017-3813-1